Macromolecules
ARTICLE

Macromolecules **2010**, *43*, 6033–6044 **6033**
DOI: 10.1021/ma100694y

Synthesis of Donor−Acceptor Multiblock Copolymers Incorporating Fullerene Backbone Repeat Units

Roger C. Hiorns,*[,†,‡,§] Eric Cloutet,[†,§] Emmanuel Ibarboure,[†,§] Abdel Khoukh,[∥] Habiba Bejbouji,[⊥] Laurence Vignau,[⊥] and Henri Cramail[§]

[†]*CNRS, Laboratoire de Chimie des Polymères Organiques, 16 avenue Pey Berland, Pessac Cedex, F33607, France,* [§]*Université de Bordeaux, Laboratoire de Chimie des Polymères Organiques, ENSCBP, Pessac Cedex, F33607, France,* [∥]*CNRS, Université de Pau et des Pays de l'Adour, 2 avenue du Président Angot, 64053 Pau, France, and* [⊥]*Université de Bordeaux, Laboratoire de l'Intégration du Matériau au Système, CNRS UMR 5218, ENSCBP, Pessac Cedex, F33607, France.* [‡]*Current address: CNRS, IPREM (EPCP, UMR 5254), Université de Pau et des Pays de l'Adour, 2 avenue du Président Angot, 64053 Pau, France*

Received March 31, 2010; Revised Manuscript Received June 4, 2010

ABSTRACT: The synthesis of the first example of a block copolymer based on a polymer using fullerene as a backbone repeat subunit is demonstrated. A facile route incorporating the electron acceptor and high fullerene content polymer, poly{(1,4-fullerene)-*alt*-[1,4-dimethylene-2,5-bis(cyclohexylmethyl ether)phenylene]} (PFDP), with the archetypal electron donor, poly(3-hexylthiophene) (P3HT), into a multiblock copolymer (MBC) structure is presented. α,ω-Bromomethyl-PFDP was prepared by atom-transfer radical addition polymerization (ATRAP) and then reacted with α,ω-phenol-P3HT via a Williamson condensation to yield the MBCs. The lengths of the electron-acceptor and donor polymer blocks could be selected so that the resulting solid state domains were of a size appropriate to organic solar cells. Also it was found that the MBCs gave a wide range of macro-structures, from micelles to well-defined wires, depending on the preparation conditions.

Introduction

Conjugated rod−coil block copolymers can yield an enormous number of well-defined nanoscale objects and structures such as vesicles,[1] and lamellae and cylindrical aggregations.[2] This extraordinary capability is enthused by the even more startling properties of the conjugated blocks that can be exploited in photovoltaics,[3] electroluminescent diodes,[4] electro-optics,[5] electronics,[6] tissue engineering, and neurology.[6e,7] This multiplicity of behavior is all the more surprising when it is found that the self-assembly process of rod−coil copolymers can be altered using a wide number of parameters such as the type of solvent, the temperature and substrate conditions.[8] One particular drive for the development of rod−coil polymers has been the current need for cheap, in other words organic, solar cells. This has pushed forward a field to the point where efficiencies around 7% have been attained using the so-called bulk-heterojunction structures,[3,9] wherein the active layer is based on a composite of an electron donating polymer and an acceptor such as [6,6]-phenyl C_{61} butyric acid methyl ester (PCBM).[10] However, still higher efficiencies and stabilities will be required to expand the available market of such materials. And frustratingly, especially when considering the exceptional properties of rod−coil copolymers, it has not been possible to incorporate the most prevalent material, *i.e.*, fullerene (C_{60}), directly into the main-chain structure to prepare the coil segments.

In polymer-based organic solar cells (pOSC), the dominant opto-electronic process is that of the polymer absorbing a photon and forming an excited electronic state termed an exciton. When this *quasi*-particle meets an interface with an electron acceptor, such as PCBM, within the mean pathway length of the exciton (understood to be from around 4 to 27 nm for P3HT), it results in electron transfer from the polymer to the PCBM.[11,12] An ensuing percolation of the thus formed hole on the polymer and the electron on the PCBM in opposite directions, via intra- and inter-macromolecular transfers, can result in a useable current. This understanding has led to a rationale for the use of block copolymers in solar cells, based on the idea that donor and acceptor blocks can self-assemble to form adjacent domains of sizes engineered for exciton capture and charge transfer.[13−20] While acceptors based on polymers have been developed, such as the first example based on a cyano-derivative of poly(phenylene vinylene) (PPV),[21] and more recently, a sulfone−alkyl derivatized PPV,[22] a major problem that many chemists have been confronted with is that, in the main, polymers preferentially conduct holes, rather than electrons.[12a,c] Accordingly, recent studies have tended to concentrate on preparing block copolymers that combine a block of poly(3-hexylthiophene) (P3HT) or poly(phenylene vinylene) as the donor, and commodity polymers carrying pendent groups such as perylene or fullerene (C_{60}) as acceptors.[20,23−29] The archetypal donor polymer, P3HT, is a useful standard for such studies as it can be synthesized with predetermined molecular weights[30] and well-defined chain ends,[31] and its electronic behavior[32] and crystallization is well characterized.[33]

Given the theoretical and demonstrated improvements that can be found when using block copolymers over bulk-heterojunction devices, it is surprising that in general solar cells made with block copolymers do not yet display properties that are better than their bulk heterojunction equivalents. While there is some debate with respect to the optimum orientation of the block copolymers to the electrodes,[15,19] for example see the proposed structure in Figure S1, Supporting Information, these points might be resolved by, incorporating C_{60} into the main-chain to make up the "coil",[34] thereby reducing the presence of electronically inert supports, and using multiblock copolymers (MBC).

*Corresponding author. E-mail: roger.hiorns@univ-pau.fr.

Published on Web 06/21/2010

Scheme 1. Synthetic Route to PFDP, P3HT, and PFDP-*b*-P3HT

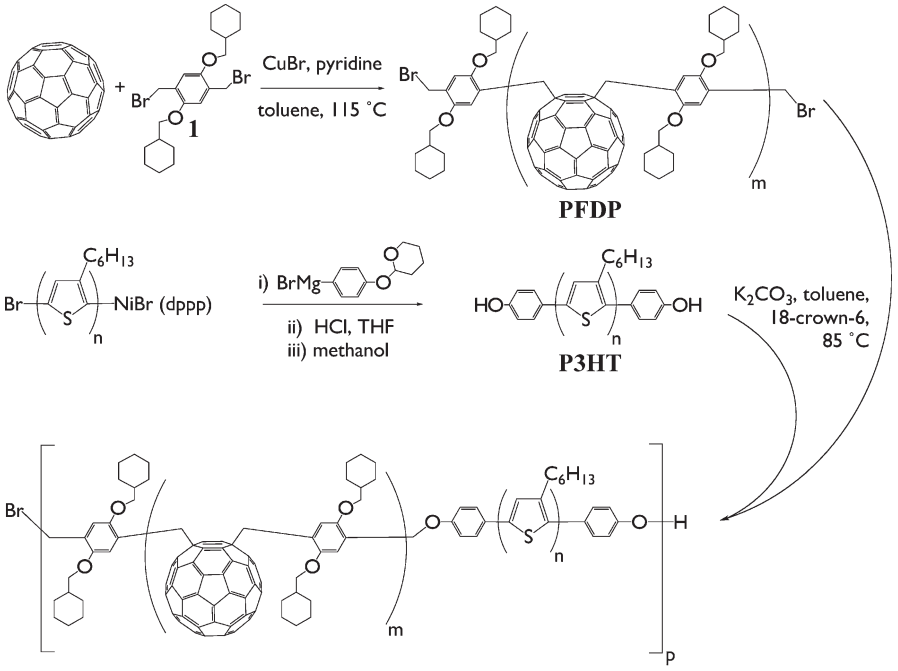

It is possible that MBCs containing conjugated segments may enforce more regular macrostructures then their di- or triblock counter parts.[1c−e,35] MBC macromolecules tend to lie parallel to the electrode due to their high length-to-width ratio and inflexibility. This geometry may enhance interactions between the electrodes and the π-orbitals of the photoactive volume. Donor and acceptor segments are covalently joined by "linker" groups that facilitate excitonic electron transfer while separating the electronic bands of each segment.[19,36]

We recently disclosed the preparation of a main-chain fullerene polymer, namely poly{(1,4-fullerene)-*alt*-[1,4-dimethylene-2,5-bis(cyclohexylmethyl ether)phenylene]}, or PFDP for short (see Scheme 1 for the structure).[34] This polymer is of interest as it is extremely facile to prepare; it does not require lengthy premodification of the C_{60} nor undergoes noticeable cross-linking, as can be the case using prior systems.[37] Given the above stated aims, and the importance of trying to incorporate C_{60} directly into the rod−coil copolymers, we thought to find out if it would be possible to perform chain-end chemistry on this extremely novel polymer to result in materials that would lead to domain formation in the solid state.

Results and Discussion

Starting Materials. *PFDP*. PFDP consists of a high proportion of propinquitous C_{60}s (*ca.* 62%) and therefore its solubility is limited with respect to concentration, although it is worth noting that it cannot be precipitated out from toluene using THF. PFDP was prepared using atom-transfer radical addition polymerization (ATRAP) of 1,4-bis(methylcyclohexyl ether)-2,5-dibromomethylbenzene with C_{60} as shown in Scheme 1.[34] In reference34, where the chemistry to form PFDP for the first time was the same as used here, ^{1}H NMR and UV−visible spectroscopies and cyclic-voltammetry indicated that the C_{60} moieties were interconnected with bis(methylcyclohexyl ether)-2,5-dimethylene benzyl groups through links across a single phenyl-like ring in the C_{60} sphere. Scheme 1 shows this link across a C_{60} phenylic ring in the 1,4-position only. Given the steric bulk of **1**, it was expected that 1,2-additions would not occur, nevertheless, from the characterizations available at that time, they could not be excluded. Results from cyclic-voltammetry (Figure 4 of ref 34) tended to indicate that if this 1,2-addition isomer were present then it would make up around 20% of the total. However, on returning to the results, it is possible that they arose from the presence of unreacted C_{60} mixed with the PFDP. It was thus felt that the characterization of the PFDP should be revisited. Recent improvements in the NMR equipment in our laboratory meant that much greater in-depth analysis of PFDP samples could be undertaken. The ^{1}H NMR of PFDP, shown in Figure S2, Supporting Information, is much like that of the last report,[34] and confirms the majority presence of 1,4-additions to C_{60}. The possibility of 1,2-additions cannot be excluded using the ^{1}H NMR because there are numerous minor peaks, a common occurrence in polymer chemistry where each atom along the chain experiences a slightly different electro-magnetic environment, and specifically to this case, the relatively poor solubility of the material leading to spikes associated with the presence of aggregates. Figure 1 shows a representative ^{13}C NMR of PFDP. It is worth noting the presence of C_{60} indicated by the peak at 143.29 ppm is exaggerated by its high solubility with respect that of the PFDP. Peaks in Figure 1 were assigned using corroborative structural information gained from the aforementioned ^{13}C DEPT NMR (Figure S3, Supporting Information), 2D HMQC ^{13}C−^{1}H NMR (Figure S4, Supporting Information)—extended by the 2D HSQC ^{13}C−^{1}H NMR (Figure S5, Supporting Information), and a 2D HMBC ^{13}C−^{1}H NMR (Figure S6, Supporting Information), the latter of which confirmed the long distance (^3J and ^4J coupling) within the repeat unit. The peaks of the PFDP can be compared with those of a model molecule, namely 1,4-diphenylmethylene fullerene bis-adduct, denoted 1,4-($C_6H_5CH_2$)C_{60}, and its isomer 1,2-($C_6H_5CH_2$)C_{60}, that have been studied in considerable detail elsewhere.[38−41] Peaks due to C_{60} sp^2 hybridized carbons are found in the region from 139.54 to 158.69 ppm. In the work by Kadish et al.[38] on the model compounds, they noted the difference between the predicted and found number of

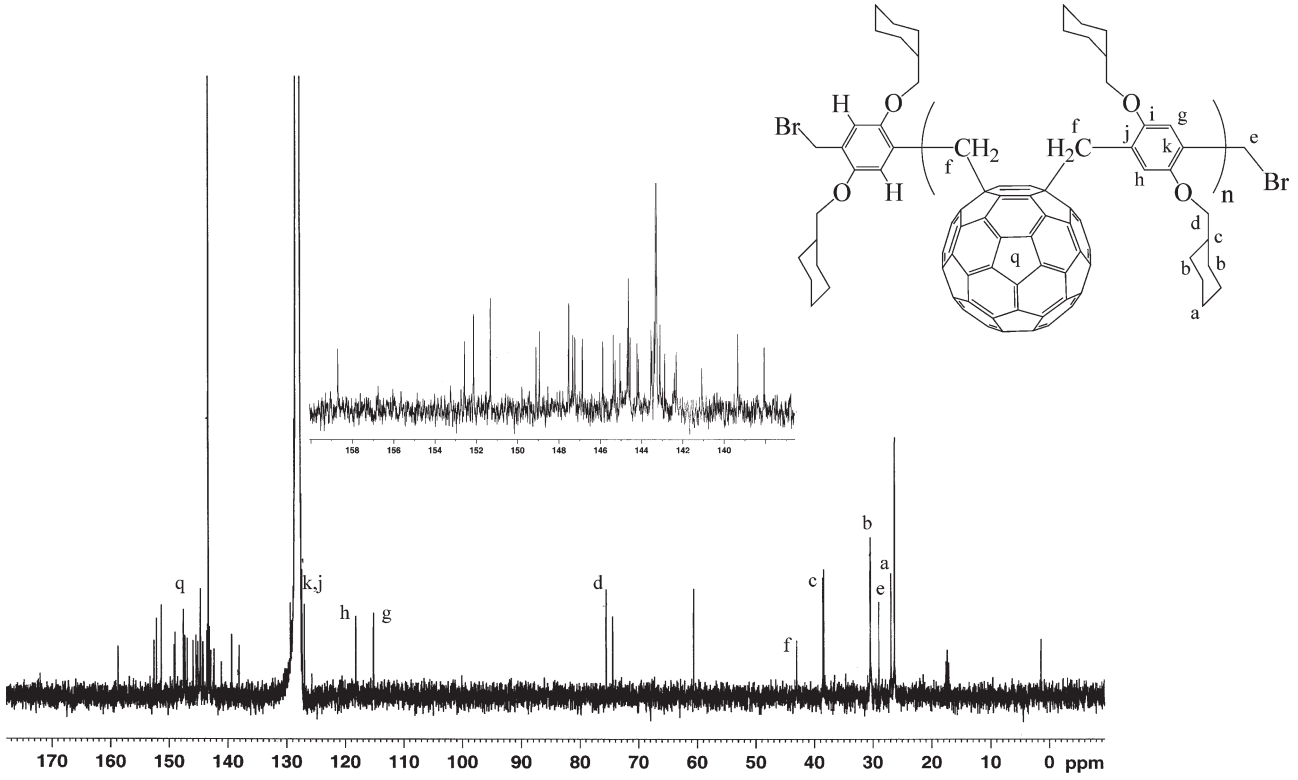

Figure 1. ^{13}C NMR (100 MHz, C_6D_6, D1 = 10 s, scans = 8192, ambient) spectrum of PFDP. Note presence of C_{60} (143.3 ppm).

peaks for both 1,4-($C_6H_5CH_2$)C_{60} and 1,2-($C_6H_5CH_2$)C_{60}, in the first case overlapping of peaks reducing their number from 31 expected to 28, and in the second arising from a reduction in symmetry (increasing from 16 to 25).[42] We found 28 peaks with a spread similar to those of 1,4-($C_6H_5CH_2$)C_{60} giving conclusive evidence for the predominance of the 1,4-addition product in PFDP. Although a small proportion of 1,2-addition PFDP products may be present, they could not be determined within the limits of experimental error. Elsewhere in the ^{13}C NMR, the phenylic sp^2 carbons at inter-C_{60} and chain-ends moieties were particularly hard to identify due to the coincidence of their small peaks (due to their poor relaxation) with large peaks arising from benzene and deuterated toluene in the NMR solvent. However, a peak at 126.98 ppm (not present in the DEPT 135° of Figure S3, Supporting Information), was assigned to an in-chain phenyl carbon close to a methylene fulleride moiety (labeled j in Figure 1). Similar poorly relaxing asymmetric phenylic carbons adjacent to ether moieties were, perhaps, visible as small peaks at 152.57 and 152.6 ppm. The sp^2 carbons with associated protons on the same phenyl rings (labeled g and h in Figures S3−S6, Supporting Information) relaxed easily to give the strong peaks at 115.15 and 118.15 ppm. The correlations of the HMQC spectrum (Figure S4, Supporting Information) of a single ^{13}C NMR peak at 43.03 ppm and the ^1H NMR double−doublet centered at 4.17 ppm are due to diastereotopic methylene groups attached to the C_{60} in a 1,4-position (as shown in Scheme 1). Their separation is again indicative of the high degree of asymmetric repulsion around the 1,4-bonds. The $-CH_2-O-$phenyl methylene carbons are clearly indicated by a peak at 75.5 ppm in the ^{13}C NMR that correlates with both the double−doublets at 3.96 ppm and the collection of minor peaks at *ca.* 3.94 in the HMQC ^1H NMR characterization, this spread being due to the polymeric nature of the material. The same spectrum indicates that the peak in the ^{13}C NMR spectrum due to $-CH_2Br$ groups is at 28.95 ppm. It is surrounded by peaks due to methylene carbons in the cyclohexyl groups at *ca.* 30.4, 28.95, and 26.86 ppm.

In accordance with the polycondensation-like nature of the reaction, the PFDPs displayed broad molecular weight distributions, as demonstrated by the GPC curves in Figure 2. Polystyrene standards could not be used for PFDP samples due to the extreme difference in exclusion behaviors, common to C_{60} based materials.[43] Indeed the M_p of PFDP was indicated, against polystyrenes, to be around 490 g mol^{-1}, a value that was clearly erroneous! The approximate peak molecular weight M_p of the PFDP, shown in Table 1, was estimated using a GPC calibrated against a crude PFDP sample, which was assumed to display peaks due to incremental increases in oligomeric masses.[34] Very low molecular weight oligomers of around 4 repeat units and less were removed during the purification process. Although it is estimable that some chains contained up to several tens of repeat units, the M_p was estimated closer to around 9 repeat units. It was found possible to fractionate PFDP using the solvent/nonsolvent pair of toluene and methanol, however, in this case, and as discussed below, the molecular weight of the received PFDP was considered appropriate for further chemistry.

P3HT. Two samples, carrying phenolic groups at both chain-ends (exampled by the ^1H NMR shown in Figure S7, Supporting Information, and the MALDI−TOF of Figure S8, Supporting Information), were prepared using well-established routes.[30,31a] Their molecular weights and dispersities ($Đ = M_w/M_n$) are given in Table 1. The number-average degree of polymerization ($\overline{DP_n}$) of P3HT-**1** was *ca.* 29 repeat units, a value low enough to facilitate chain-end chemistry but also low enough to perhaps invoke chain-confinement effects and limit inter-P3HT electronic interactions.[30d,33c,44−46] P3HT-**2** had a higher molecular weight ($DP_n \approx 36$) and was expected to form greater intermacromolecular interactions.

Multiblock Copolymer Formation. It was planned to have near equal volumes of PFDP and P3HT segments. It is

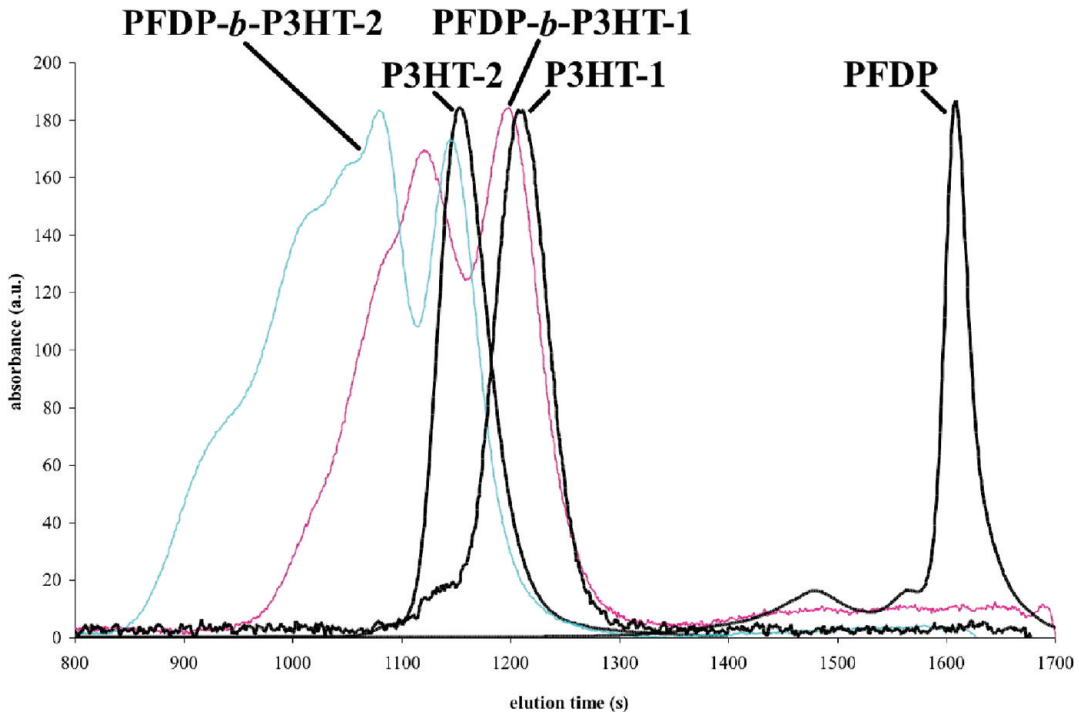

Figure 2. Normalized GPCs (UV 254 nm, THF) of the homopolymers and their associated copolymers.

Table 1. Characteristics of the P3HTs, PFDPs, and Resulting MBCs in This Study

sample name	M_p (g mol^{-1}, GPC)[a]	M_n (g mol^{-1}, GPC)[a]	$Đ$ (GPC)	$\overline{DP}$[b]
PFDP	9930		high	9
P3HT-**1**	7925	7965	1.05	*ca.* 29
P3HT-**2**	11 880	10 690	1.07	*ca.* 36
PFDP-*b*-P3HT-**1**	30 130	23 530	2.4	—
PFDP-*b*-P3HT-**2**	26 060	25 750	5	—

Notes: [a] In the case of PFDPs, calculated against peaks due to incremental increases in the molecular weights of oligomers found in the crude PFDP; and in the case of P3HTs, calculated against polystyrene standards and therefore to find the "actual" values, those shown in the table should be divided by a coefficient of between 1.6 and 2.3.[31c] It should be noted that in the case of PFDPs, MALDI−TOF conditions were found to yield only values corresponding to single units due to the relatively facile rupture of the $-CH_2-C_{60}$ bond under MALDI−TOF conditions (see ref 34); in the case of P3HTs, these values may give underestimations of "real" molecular weights due to easier "flight" of lower molecular weight macromolecules; and in the case of PFDP-*b*-P3HTs, it was not found possible to obtain results. [b] Calculated for P3HTs using the graph in Figure 4 of ref 31c and for PFDPs against PFDP calibrated GPCs.

generally recognized that block copolymers preferentially select lamellae domain structures when the block volumes are equivalent, although the final orientation and structure are environment (substrate, film thickness, *etc.*) sensitive.[47,48] It should be noted also that polymers containing conjugated segments tend to have phase diagrams that prefer lamellae formation over a wider range of block volume ratios with a tendency toward hexagonal formations only when asymmetric block volumes are used, probably due to their tendency toward linearly organized crystallization.[49]

The size of the domains are defined to a great extent by the maximum mean pathway limit of the excitonic state (*ca.* between 4 and 27 nm),[11−13,19,26] and the minimum confinement length of the P3HT block. The former implies that the P3HT chain should not be more than 27 nm/0.38 nm (where 0.38 nm is the inter-3HT repeat unit distance[50]) ≈ 70 units long, and the latter that is should not be far less than the aforementioned 29 units. The actual samples received are in effect at the lower limit (P3HT-**1** at *ca.* 29 units giving a chain length of *ca.* 11 nm) and near midway between known exciton pathway limits (P3HT-**2** with $\overline{DP_n} \approx 36$ has a chain length of *ca.* 14 nm).

In order to attain an equivalence of volumes in the P3HT and PFDP blocks, assuming that the P3HT samples do not fold, P3HT-**1** and P3HT-**2** would require that the PFDP blocks, respectively, take up around $29 \times 0.38 \times 0.38 \times 1.6 = 6-7$ nm^3, and *ca.* 9 nm^3 (using values from refs 50 and 51). Given that the volume of C_{60} is around 1 nm^3,[52] and that the inter-C_{60} groups are relatively small, it would seem apparent that PFDPs with volumes of around 5 and 8 nm^3 would thus be required to copolymerise with P3HT-**1** and P3HT-**2**, respectively. The actual received $\overline{DP_n}$ of the PFDP was of this order, and therefore no effort was made to fractionate it.

In order to attain an MBC, the Williamson polycondensation reaction of α,ω-dibromomethyl-PFDP and α,ω-diOH-P3HT shown in Scheme 1 was chosen above other possible routes for its ease and simplicity. The presence of the C_{60} moiety excludes some anionic and radical chemistry and therefore the nucleophilic attack of the hydroxyl group to the labile methyl bromides was thought to be the most appropriate route. In addition, it was thought that a flexible methylene ether link between PFDP and P3HT might ensure a separation of the respective electronic band structures while maintaining their physical proximity[19] and facilitate crystallization within each domain by alleviating dense packing at the interface.[53] Various conditions were attempted, for example in the presence of KI, and/or pyridine, but these reactions resulted in the formation of insoluble products that arose from cross-linking. It was found that the reaction performed in the presence of K_2CO_3 and 18-crown-6 was the most efficient. With both P3HT-**1** and P3HT-**2**, and as indicated in Figure S9, Supporting Information, the formation of block copolymers was quite rapid (under 7 min, a not unusual occurrence *per se*) but that in order for all the starting materials to react, a considerably greater amount of time was required—probably due to physical effects such as aggregation of the rapidly increasing molecular weight

MBCs increasing viscosity and, in effect, "hiding" chain-ends from reactions—a common problem with rod−coil MBC formation.[1e] Although high yields of these quickly prepared crude products could be obtained (*ca.* 70%), it was found to be extremely difficult to remove unreacted P3HT either using selective solvents with a Soxhlet or fractionation by precipitation. Given that for this study it was felt interesting to explore the pure material, the reactions were thus left to run to completion (which invited the formation of extremely high molecular weight aggregates due to secondary reactions as demonstrated in Figure S9, Supporting Information), and then the aggregates were filtered off. This was found to be the simplest method to obtain the pure block copolymers of poly{(1,4-fullerene)-*alt*-[1,4-dimethylene-2,5-bis(cyclohexylmethyl ether)phenylene]}-*block*-poly(3-hexylthiophene) and denoted PFDP-*b*-P3HT-**1** and PFDP-*b*-P3HT-**2**, the GPCs of which are shown in Figure 2.

Given that the PFDP exhibits an overly long GPC exclusion time with respect to its actual mass (for example an M_p of around 9000 g mol^{-1} in PFDP appears as around 490 g mol^{-1} against polymer standards), the reactions forming the di- and triblock copolymers (PFDP-*b*-P3HT and PFDP-*b*-P3HT-*b*-PFDP) will result in GPC peaks not far from the initial P3HT starting material. This can clearly be seen in Figure 2 for the lower order reaction products of PFDP-*b*-P3HT-**1** and PFDP-*b*-P3HT-**2**. Further additions of P3HT to the chain result in much greater changes in the MBC exclusion times. However, each subsequent shoulder is relatively broad; it is reasonable to suppose that while the exclusion time is dominantly determined by the number of P3HTs in the MBC, each shoulder envelopes MBCs with two, one or zero PFDPs at the chain-ends.

The aforementioned cross-linking, found when long reactions times were used, might have been due to secondary reactions between activated phenolic chain-ends (Ph−O$^-$ K$^+$) and C_{60} moieties in the PFDP. The literature details that C_{60} has been shown to be unable to quench oxanions.[54−56] Prior work has, nevertheless, found that these secondary reactions may occur to a limited extent,[57] and it is probably these that were slowly leading to the formation of the high molecular weight aggregates. That the cross-linking might have been due to Gilch-like reactions between PFDP chain-ends was excluded as such a step would require the presence of two methyl halide groups on each chain-end phenyl ring to form the requisite α-bromo-*p*-quinodimethane starting unit.[58,59]

An ^{1}H NMR experiment with the block copolymer was attempted, however, results were limited by the relatively low solubility of the PFDP segment of PFDP-*b*-P3HT in the available deuterated solvents. Peaks were identified associated with the presence of PFDP (see Figure S10, Supporting Information) and indeed probably with links between PFDP and P3HT (detailed in Figure S10, Supporting Information), but of a highly reduced amplitude due to the aggregation of the PFDP blocks in the solvent at the requisite NMR experiment concentration.

Thermal Characterizations. Figure S11, Supporting Information, shows the representative thermal gravimetric analyses (TGA) of the individual blocks, P3HT-**1** (curve a), PFDP (b), and of the copolymer PFDP-*b*-P3HT-**1** (c). P3HT-**1** exhibits a non-negligible (2% loss) degradation from about 400 °C and reaches a plateau with a midpoint at *ca.* 620 °C following a loss of *ca.* 58% mass. This is ascribed to the loss of hexyl side-chains.[60] In the case of PFDP, the same 2% loss arrives at a lower temperature (*ca.* 280 °C), most likely due to chain-end bromines. At higher temperatures there is a gradual loss of cyclohexyl groups due to the presence of thermally unstable ether links.[61] There is a major plateau in the degradation with a midpoint at *ca.* 470 °C (*ca.* 17% weight) which is close to the expected 18% weight loss that would be expected with the removal of all cyclohexyl groups. The thermal degradation of PFDP-*b*-P3HT-**1** shows, as expected, a combination of the two prior curves. The loss of cyclohexyl groups at *ca.* 450 °C contributes to a 9% loss in weight, indicating that the PFDP makes up around 53% (9/17 × 100%) by weight of the block copolymer. The rest of the curve, including the midpoint of the second plateau in the curve at *ca.* 540 °C (*ca.* 49% loss) resembles a combination of the two curves of the component blocks and is due to a combined loss of the aforementioned cyclohexyl moieties, P3HT hexyl side-chains and PFDP chain-units. The temperature required for the loss of the P3HT hexyl side-chains along with the main chains of both polymers is reduced by the order of at least 50 °C for the P3HT block and around 120 °C for the PFDP block, indicating that in the unorganized solid state both blocks are mutually perturbed.

The representative DSC curves of the starting materials, PDFP, P3HT-**1** and PFDP-*b*-P3HT-**1**, are shown in Figures S12a and S12b, Supporting Information. Figure S12a, Supporting Information, shows the first heating and cooling passages, while Figure S12b, Supporting Information, shows the same samples going through their second heating and cooling cycles. While it is accepted that the first passage is not widely used due to the discrepancies that may be introduced by a "thermal history", that is a microstructure resulting from uncontrolled thermal treatments and disparate precipitations, we found that the curves were repeatable across different samples, hence the following discussion based on the difference between the first and second curves of these materials. With the molecular weight of P3HT-**1** being relatively low, the value of the apparent melting temperature (first cycle, T_m = 207 °C, ΔH_m = 27.4 J g^{-1}; second cycle, T_m = 205 °C, ΔH_m = 22.4 J g^{-1}) is lower than the *ca.* 240 °C quoted elsewhere,[62] and due to the decrease in T_m with molecular weight.[63] On cooling, a crystallization peak appears (1st cycle, T_c = 182 °C, ΔH_c = 22.7 J g^{-1}; second cycle, T_c = 184 °C, ΔH_c = 21.0 J g^{-1}). It is therefore interesting to consider the degree of crystallinity in the samples prior to and following the first melting by taking ΔH_m and dividing it by the specific heat of melting for a 100% crystalline sample of P3HT ($\Delta H_{0(P3HT)}$ = 99 J g^{-1}), for the first and second passages.[64] The respective values obtained are thus 23% and 21% and are in accordance with those found elsewhere.[64] Given that the second passage was slower than the first, it should exhibit a greater degree of crystallization, however, the formation of small, trapped crystallites that restrict macromolecular movement in the first passage perturbed the second characterization and led to a decrease in the observed values. In the case of the PFDP, there is a broad endothermic peak at around 270 °C due to some reorganization, perhaps related to the slight degradation detailed above. It is only slightly visible on the second passage, and given that this event has been observed for other samples,[34] it is probable that it is due to an irreversible increase in order in the material. It would also tend to indicate that the C_{60}s are proximate enough to take on a more stable structure, either intra- or intermacromolecularly, even in the presence of the cyclohexyl rings. This is not surprising given the considerable size of the C_{60} with respect to the inter-C_{60} moieties. For PFDP-*b*-P3HT-**1**, the curve displays a T_m at *ca.* 192 °C (ΔH = 4.8 J g^{-1}), with an onset at 160 °C, *i.e.* much broader and lower than that for the pure P3HT. This peak is due to a P3HT that has had its morphology disorganized by the presence of the PFDP. The descent in temperature reveals a peak at 103 °C (ΔH_c = 0.6 J g^{-1}, indicating *ca.* 0.6% crystallinity) due to P3HT, which being lower than that of the pure P3HT-**1** confirms, with the TGA results, that the

P3HT in PFDP-*b*-P3HT-**1** is structurally perturbed by the PFDP. This dispersion of the P3HT chains is caused by their being covalently bound to the PFDP which restricts movement at the chain-ends, and is a barrier to crystallization along the chain-length. This effect has been observed for other block copolymers of P3HT, notably that of poly(3-hexylthiophene)-*block*-polyethylene, where the aggregation of the polyethylene has hampered the crystallization of the P3HT.[64a] This idea is reinforced by the second heating and cooling passages of PFDP-*b*-P3HT where the P3HT undergoes only very slight melting and crystallizing; its structuration is now restricted by the PFDP which may itself have undergone an irreversible organization.

UV−Visible Characterizations. Figure 3 shows the UV−visible absorption characterizations of equiweight solutions of P3HT-**1**, PFDP, PFDP-*b*-P3HT-**1**, and PFDP-*b*-P3HT-**2** in toluene. The absorption curve for P3HT-**1**, with a λ_{max} at 450 nm (1.125×10^{-4} g L^{-1}, *ca.* 2.3×10^{-6} mol L^{-1}, ε = 223 000 L mol^{-1} cm^{-1}), is comparable to samples found elsewhere,[65] and it is considered representative of both P3HT-**1** and P3HT-**2**. The absorption curve for PFDP is similar to (if slightly shifted from) that of C_{60}, most notably in the strong absorption at 334 nm and a minor peak at around 406 nm. A similar correlation has been observed elsewhere for 1,4-bis adducts.[41] However, unlike C_{60}, PFDP in toluene gives rise to deep red color. Its curve contains a weak absorption centered around 445 nm, which is considered diagnostic of a C_{60} 1,4-addition product.[39,66] The zoom shows a tailing in the absorption curve at higher wavelengths, with "bumps" at 598 and 694 nm that are typical to addition products of C_{60}.[38] The UV−visible curves of the PFDP-*b*-P3HT-**1** and PFDP-*b*-P3HT-**2** resemble a combination of those of PFDP (at 334 nm) and P3HT (at 450 nm), indicating that there is no mixing of P3HT HOMOs and PFDP LUMOs, *i.e.*, each segment retains its own band structure. Although not absolutely correct due to the possibility of changes in conformations with concentration and the necessary assumption that at the P3HT λ_{max} the PFDP makes a negligible contribution, an estimation may be made to the relative weight of P3HT in each copolymer through a simple division of the absorbance due to P3HT at the λ_{max}, as the concentrations of the solutions are *all* at 1.125×10^{-4} g L^{-1}. This simple reckoning gives the weight of P3HT in PFDP-*b*-P3HT-**1** as $(0.2808/0.5120) \times 100\% \approx 55\%$ and in PFDP-*b*-P3HT-**2** as $(0.2333/0.5120) \times 100\% \approx 45\%$. This result corroborates that given by the TGA, at least within the order of error. Further confirmation of the incorporation of PFDP into the copolymers is given by the extension of the absorption curve to around 730 nm; a value not reached by P3HT alone and characteristic of PFDP. It is notable that here the absorbance of PFDP-*b*-P3HT-**2** is slightly stronger than that of PFDP-*b*-P3HT-**1** from *ca.* 600 to 730 nm. This is due to the greater incorporation of PFDP in PFDP-*b*-P3HT-**2**. It should be noted that the absorbance of this peak at 730 nm varied proportionately with other peaks associated with PFDP at various concentrations, confirming that it was due to macromolecules rather than aggregative effects.

Fluorescence Characterizations. Characterizations of MBCs and their component blocks were performed at the same temperature, range of concentrations (at and less than 5 μg mL^{-1} to minimize reabsorption phenomena) and excitation wavelength (450 nm, *i.e.*, at the λ_{max} of P3HT-**1**) permitting direct comparisons to be made between samples.[67] PFDP, at the concentrations used, emitted near negligible fluorescence at this wavelength. P3HT-**1** exhibited a typical emission spectrum with a λ_{max} at 576 nm, and two minor shoulders at around 615 and 700 nm (Figure S13, Supporting Information). These

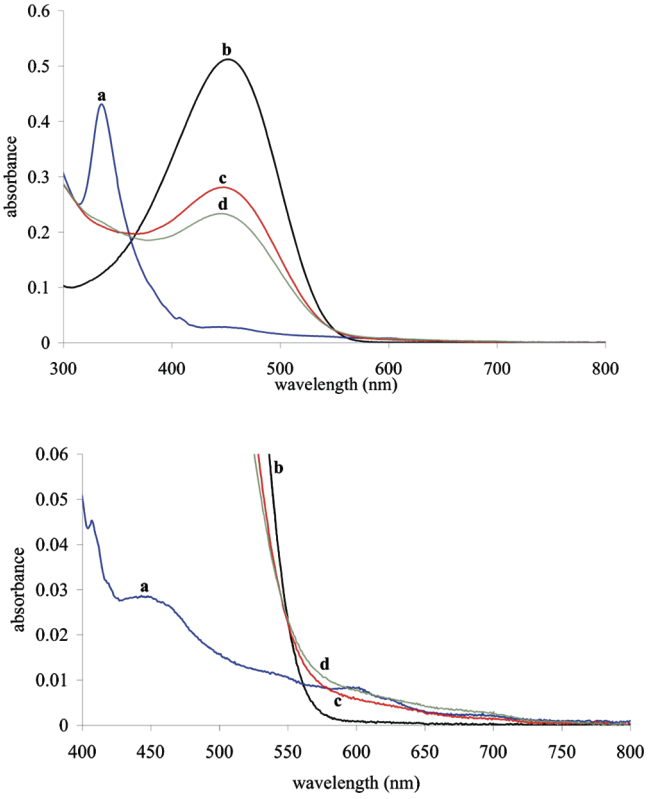

Figure 3. UV−visible characterizations all in toluene at ambient temperature and at concentrations of 11.25 μg mL^{-1}, where the image below is a zoom from the image above: (a) PFDP; (b) P3HT-**1**; (c) PFDP-*b*-P3HT-**1**; (d) PFDP-*b*-P3HT-**2**.

characteristics did not change on incorporation into PFDP-*b*-P3HT-**1**, indicating that there is no change in the band structure of the P3HT segment on being covalently bonded to the PFDP, something that is expected given that the methylene (oxide) link between P3HT and PFDP would not permit band mixing.[19] However, at equal concentrations, the fluorescence of P3HT was reduced by *ca.* 80%, rather than around 45% as would be expected from the aforementioned UV−visible results alone. This result would tend to indicate that there is a strong quenching of the emission from P3HT by the PFDP in the MBC. As Figure S14, Supporting Information, shows, the fluorescence intensity of PFDP-*b*-P3HT-**1** follows a typical variation with reduction in concentration,[68] but at all stages remains considerably less than an equivalent solution containing equi-weight amounts of the homopolymers PFDP and P3HT-**1**. This result would tend to confirm the effectiveness of the fluorescence quenching, and hence probable electron transfer from one to the other, provided by the proximity of the two blocks in PFDP-*b*-P3HT-**1**.

AFM. While the above characterizations center on PFDP-*b*-P3HT-**1**, considered representative for PFDP-*b*-P3HT-**2**, the following studies concentrate on PFDP-*b*-P3HT-**2** as it was found to be difficult to attain comparable organisations for PFDP-*b*-P3HT-**1**, probably due to the shorter length of the P3HT restricting macromolecular movement.

Here we wished to explore the effects of various substrates and solvents on the resulting spin-cast structures obtained from this extremely novel block copolymer. Figure 4 shows the surfaces of PFDP-*b*-P3HT-**2** thin films spin-cast onto poly(3,4-ethylene-dioxythiophene)-*blend*-poly(styrene sulfonate) (PEDOT-*blend*-PSS) supports from concentrated solutions in 1-chloronaphthalene (10 mg mL^{-1} prior to filtering). Parts a and b of Figure 4 show the surface as cast and indicate

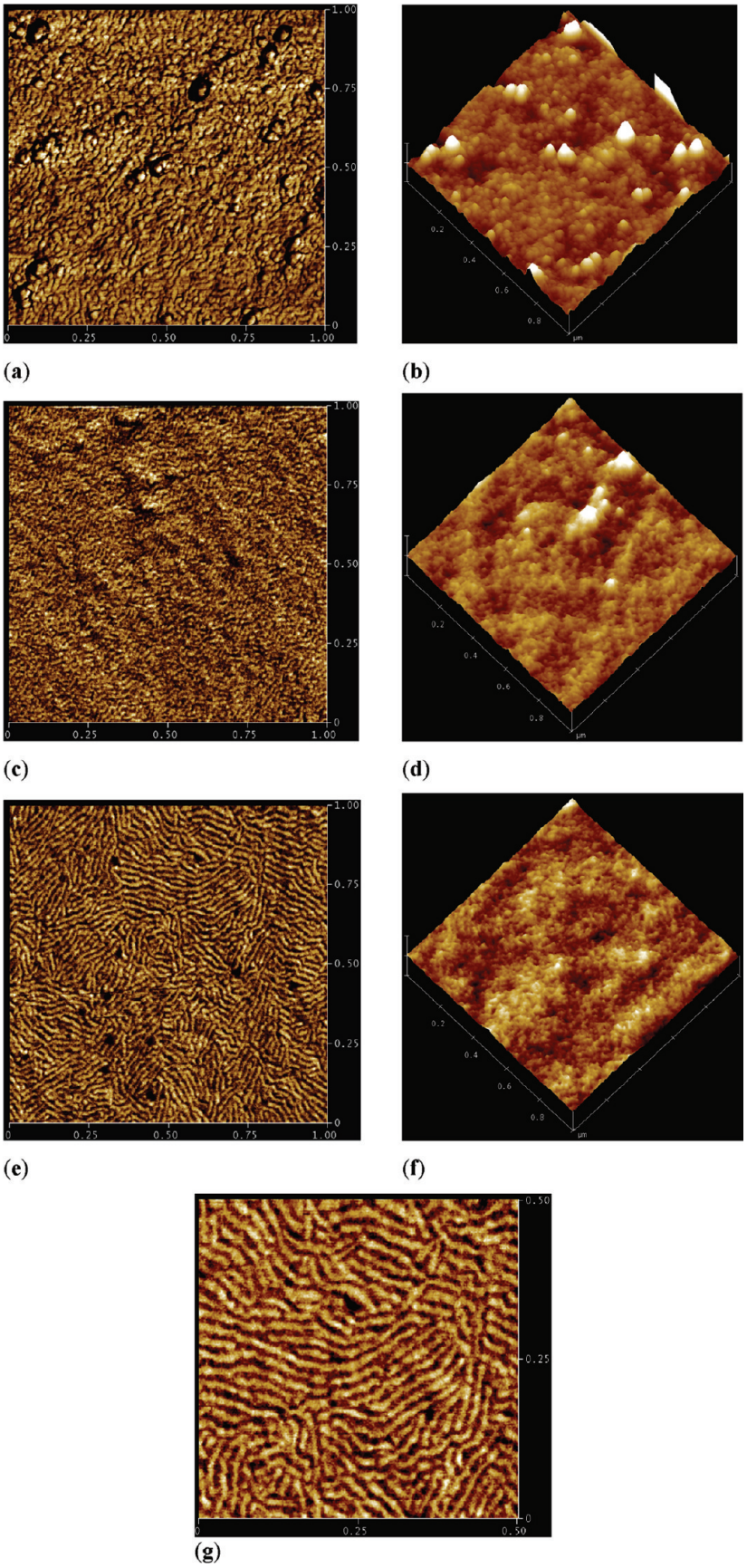

Figure 4. AFM tapping mode (phase left, height right) images of PFDP-*b*-P3HT-**2** thin films (*ca.* 140 nm thick) spin-cast from concentrated (20 mg mL^{-1}) solutions in 1-chloronaphthalene on to PEDOT-*blend*-PSS supports: (a) film left at 25 °C once cast (0−15° scale); (b) corresponding to part a (0−12 nm zenith); (c) phase, film annealed at 180 °C for 5 min (0−6°); (d) corresponding to part c (0−12 nm); (e) phase (0−4°) film annealed at 220 °C for 5 min; (f) height (0−12 nm) corresponding to part e; (g) phase (0−5.7°) of same sample as in parts e and f. All at 1 × 1 μm, except sample g at 500 × 500 nm.

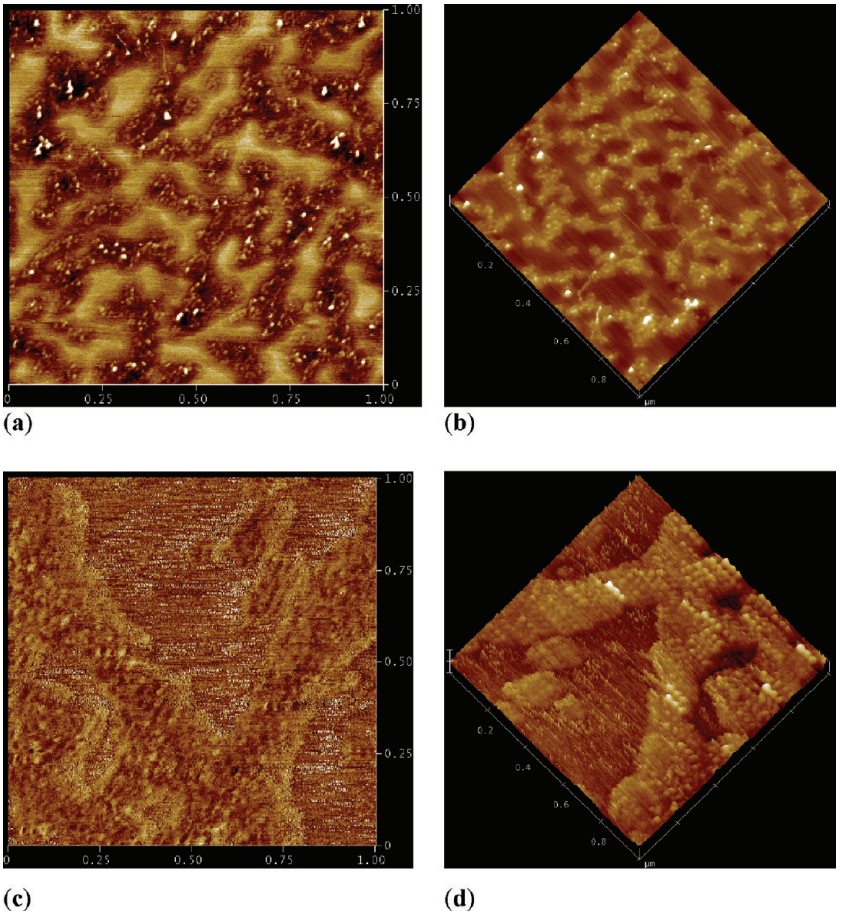

Figure 5. AFM tapping mode (phase left, height right) images of PFDP-*b*-P3HT-**2** spin-cast from dilute (0.01 mg mL^{-1}) solutions in 1-chloronaphthalene onto graphite supports: (a) film left at 25 °C once cast (0−20° range); (b) corresponding to part a (0−4 nm zenith); (c) film annealed at 160 °C for 5 min (0−15°); (d) corresponding to part c (0−4 nm). All images 1 × 1 μm.

the immediate orientation of the polymers probably into lamellae structures. However, the domains, which have a repeat unit size of *ca.* 21.5 nm (as profiled in Figure S15, Supporting Information), appear relatively disorganized and the surface is occasionally ruptured by larger blobs (around 8−14 nm in height and *ca.* 60−70 nm wide) that are due to the strong aggregation properties of PFDP-*b*-P3HT-**2** in solution, confirming the indication of the aforementioned ^{1}H NMR characterizations of the copolymer. Once annealed at 180 °C, as shown in Figure 4, parts c and d, a more regular structure can be ascertained, and it is indicated that the polymers has started to reptate and permit a more even structure. The root mean surface (rms) has accordingly reduced from 1.433 to 0.793 nm. A considerably better degree of organization though is reached (Figure 4, parts e−g) when the annealing temperature is at 220 °C, *i.e.*, above the melting point of the P3HT, as greater movement of the P3HT block around the relatively immobile PFDP segments can be attained. This may indicate that a larger and more flexible group between the PFDP and the P3HT would be required in order to permit greater crystallization of the P3HT. Accordingly the rms is further reduced to 0.457 nm, indicative of a continually effective annealing with the increase in temperature. The domain repeat unit is now slightly reduced from that of the unannealed system and is of the order of 19 nm (averaging over nine repeat units, Figure S16, Supporting Information). This is in close proximity to what was expected for PFDP-*b*-P3HT-**2**. The P3HT-**2** block was expected to be around 14 nm long and would thus lead to a domain width of that order. The PFDP could thus be around 5 to 6 nm wide, as would be expected from the number of C_{60}s it contains, which due to the geometry of the molecular structure would not all be linearly placed. Comparing Figure 4e and Figure 4f, it is apparent that it is the harder PFDP[34] which rises above the mean surface level and would tend to indicate a greater phobicity of this material with respect to the underlying PEDOT-*blend*-PSS substrate. This may have implications for the type of photovoltaic diode structure that would optimize the characteristics of PFDP-*b*-P3HT. Given the domain formation, it would be expected that the aforementioned DSC results would have indicated some crystallization of the P3HT within the domains, however, this was not obtained probably due to a geometrical restriction placed on the P3HT by the quickly aggregating PFDP, as discussed above in the section on DSC characterizations. It is also possible that there was incomplete demixing of the two domains. Again, improvements might be sort by increasing the flexibility of the electronically inert block-linking groups thus permitting greater separation of the two blocks. It should be noted that while we were unable to find indications of free C_{60} in PFDP-*b*-P3HT, and especially given the high degree of purification its presence would be unexpected, its presence cannot be excluded.

The tendency of the PFDP to control the degree of organization in these systems was explored by using dilute solutions of PFDP-*b*-P3HT-**2** (0.01 mg mL^{-1} prior to filtering). First we attempted using 1-chloronaphthalene as the solvent and graphite as the substrate. The surface coverage was quite poor, as shown in Figure 5, parts a and b; however, on heating, it was found that the system underwent an epitaxial growth, aligning with the substrate graphite (Figure 5, parts c and d).

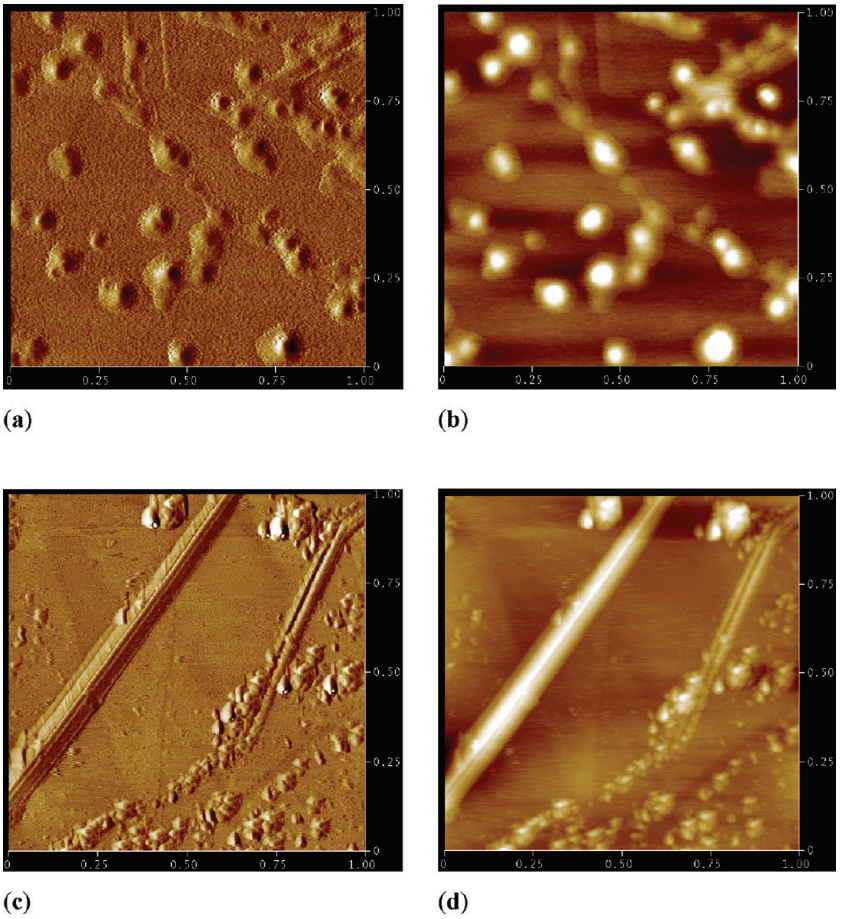

Figure 6. AFM tapping mode (phase left, height right) images of PFDP-*b*-P3HT-**2** spin-cast from dilute (0.1 mg mL^{-1}) solutions in toluene onto freshly cleaved mica supports: (**a**) film left at 25 °C once cast (0−10° range); (b) corresponding to part a (0−10 nm zenith); (c) film annealed at 170 °C for 5 min (0−10°); (d) corresponding to part c (0−15 nm). All images 1 × 1 μm.

Within each growth, it is possible to visualize a repeat unit of around 30 nm (see Figure S17, Supporting Information), close but slightly larger than that expected, due to effective spreading of the PFDP segments over the graphite surface, indicating a proximity of surface energies of the graphite and the PFDP. This effect was confirmed in the low rms values found for the unannealed and annealed surfaces (respectively 0.332 and 0.301 nm), considerably less than those found on PEDOT-*blend*-PSS substrates as noted above. To further exaggerate the effect of the PFDP in the copolymer and to explore its aggregative effects, we then attempted to use dilute solutions of PFDP-*b*-P3HT-**2** in toluene (0.01 mg mL^{-1} prior to filtering) and spread them on mica. Figures 6a and b indicate that the copolymers aggregated as micelles in solution,[62] to fall-out as structures resembling fried eggs, with the P3HT encircling blobs of PFDP as objects around 80−100 wide. The PFDP "yolk" is around 6 nm high (as indicated in Figure S18, Supporting Information), and would tend to suggest a rather good affinity of PFDP-*b*-P3HT-**2** for freshly cleaved mica. On annealing to 170 °C, below the P3HT melting point, it was found that the PFDP-*b*-P3HT-**2** could move across the surface to self-organize into wires (Figures 6c and d, and Figure S19, Supporting Information). In some cases these wires paired up to have a separation of around 10−15 nm—close to the expected domain width created by P3HT—and in others to give fibrillated large wires. This would tend to suggest that parallel wires from such materials are feasible, although there is a fine balance to be struck between the strong tendency of the PFDP to self-aggregate and control the whole system and the aggregation of the P3HT which, as part of the MBC, can make the system more linear. This formation of wires is not unlike that recently seen with modified C_{60},[52] however, in our work, this is the result of a combination of n- and p-type structures in a rod−coil block copolymer.

Conclusion

This work has demonstrated by way of using the archetypal homopolymer P3HT that it is possible to access, in a facile manner, multiblock copolymers with the novel fullerene containing polymer PFDP. This is the first example, to our knowledge, of a block copolymer that incorporates one block based on main-chain fullerene subunits. The reaction conditions can be modified simply to attain varying degrees of purity and yields. In the dispersion- and solid-states, it is apparent that it is the aggregative behavior of the PFDP that dominates the self-assembly of the system, although this may be changed through a facile modification of the inter-C_{60} moieties. Given that this block copolymer forms domains of excitonic scale, and that emission quenching between bonded blocks is demonstrated to be greater than that of unbonded blocks, it would be expected that this material should be of interest for photovoltaic devices. However, it is also expected that this material might find applications in other fields given its unusual ability to form micelles and highly linear donor−acceptor wire-like structures. In any application, though, particular care will have to be taken in the choice of substrates and casting solvents given the apparent sensitivity of PFDP-*b*-P3HT to these parameters.

Experimental Section

Apparatus. ^{1}H (400 MHz) and ^{13}C (100 MHz) NMR spectra were recorded on a Bruker Avance 400 spectrometer. Predictive

^{13}C NMR software, obtained from Advanced Chemistry Development, was used to assist peak assignments. Gel permeation chromatography (GPC) was performed using THF as eluant at 40 °C and flow rate of 1 mL min^{-1} through four columns (TSK G5000HXL (9 μm), G4000HXL (6 μm), G3000HXL (6 μm), and G2000HXL (5 μm)) and connected to Varian refractometer and UV−visible spectrophotometer calibrated against linear polystyrene (PS) standards for use with P3HT and P3HT-containing copolymers. TGAs were performed with a Perkin-Elmer TGA 7 Thermogravimetric Analyzer under nitrogen from ambient temperature to 900 °C at a heating rate of 10 °C min^{-1}. A TA DSC Q100 series calorimeter from TA Instruments under nitrogen was used to obtain curves from 10 to 300 °C at heating and cooling scan rates of 20 °C min^{-1} on the first passage and then again on a second passage at 10 °C min^{-1}. UV−visible absorption and fluorescence spectra were recorded at ambient temperature from solutions of PFDP, P3HT, or PFDP-*b*-P3HT in toluene using quartz 10 mm wide cells using, respectively, a Varian Cary 100 Scan UV−visible spectrophotometer and a Varian Cary Eclipse fluorescence spectrometer. Matrix assisted laser desorption ionization time-of-flight mass spectrometry (MALDI−TOF) was performed on an Applied Biosystems Voyager mass spectrometer equipped with a pulsed N_2 laser (337 nm) and a time-delayed extracted ion source. Spectra were recorded in the positive-ion mode using the reflectron and with an accelerating voltage of 20 kV. Samples were dissolved in toluene at 1 mg mL^{-1} and mixed with a matrix solution prepared using *trans*-2-[3-(4-*tert*-butylphenyl)-methyl-2-propenylidene]malonitrile (10 mg) in CH_2Cl_2 (1 mL) and a cationisation agent (NaI in methanol at 10 mg mL^{-1}) at the respective ratio of 10:1:1 by volume. Several μL of the obtained solution was deposited onto the sample target and vacuum-dried.

Thin films were prepared of PFDP-*b*-P3HT from 0.01 or 10 mg mL^{-1} solutions in 1-chloronaphthalene or toluene and spin-coated at 1500 rpm for 60s following an acceleration of 1.5 s for 40 s onto either predried films of PEDOT-*blend*-PSS, graphite, or mica as indicated above. Atomic force microscopy (AFM) was performed under air at 25 °C using a Nanoscope IIIa microscope operating in tapping-mode. The probes were commercially available silicon tips with a spring constant of 42 N m^{-1}, a resonance frequency of 285 kHz, and a typical radius of curvature in the 8−10 nm range. Both topography and phase signal images were recorded at a resolution of 512 × 512 data points.

Materials. C_{60} (99.9%) was obtained from MER Corporation (USA). All other materials were obtained from Aldrich (France) and used as received. Solvents were distilled from over their respective drying agents under dried nitrogen. K_2CO_3 was dried at 135 °C under reduced pressure for 24 h following washing with THF and its coevaporation of water. All reactions were performed in flame-dried and dry nitrogen flushed glassware. Where possible air and light were excluded from the reactions and the handling of polymers in solution.

α,ω-diOH-P3HT (P3HT-1 and P3HT-2). Monomers were prepared as detailed elsewhere.[31f,69] The polymerization was performed following that given elsewhere.[31a] For the sake of completeness, a representative protocol is given here. Into a 500 mL flask equipped with a stirring bar was stirred for 2 h at 25 °C a mixture of 2,5-dibromo-3-hexylthiophene (1.84 × 10^{-2} mol), THF (36 mL) and *tert*-butylmagnesium chloride (1 M in THF, 18.4 mL, 1.84 × 10^{-2} mol). The solution was then diluted with THF (120 mL) prior to the one-shot addition of 1,3-bis(diphenylphosphino)propane nickel(II) chloride [Ni(dppp)Cl$_2$] (4.04 × 10^{-4} mol). The polymerization was left stirring for 30 min, and then terminated by the addition of 4-(2-tetrahydro-2*H*-pyranoxy)-phenylmagnesium bromide in THF (0.5 M, 30 mL, 0.015 mol). After the mixture was stirred overnight, 4 mL of HCl (concentrated) was added to ensure complete termination. The solution was dropped into methanol (600 mL) and filtered into a Soxhlet thimble. The purple polymer was Soxhlet washed with methanol, then hexane, and Soxhlet recovered with THF. The THF solution of the polymer was stirred overnight with 12 drops of HCl (conc.) at 70 °C. The polymer was then precipitated three times from THF in methanol and recovered over a glass frit. Yield of P3HT-**1** was 0.64 g, 21%. GPC (THF, detector at 254 nm, against polystyrene standards): M_p = 7925; M_n = 7965; M_w/M_n = $Đ$ = 1.05. Estimated "real" values, to account for difference between polystyrene and P3HT exclusion volumes indicated by ref 31c that $M_n \approx 4900$ g mol^{-1}, equivalent to *ca.* 29 units. MALDI−TOF (see Figure S8, Supporting Information for further details, m/z [M$^+$]: M_p = 5006.9 g mol^{-1} (calc. 5007.4 g mol^{-1} for $C_{302}H_{416}O_2S_{29}$ *i.e.* Twenty-nine repeat units and 2 phenolic chain-ends). ^{1}H NMR (400 MHz, $CDCl_3$, ambient temperature): 7.52 (s, 0.35 H), 7.34 (d, J = 8.4 Hz, 2.4 H), 6.98 (s, 19 H), 6.89 (d, J = 8.8 Hz, 2.5 H), 2.81 (t, J = 7.4 Hz, 37 H), 2.62 (t, J = 7.8 Hz, 4 H), 1.5 (m, 240 H), and 0.91 (m, 65 H). Integrals should be treated with great caution due to differences in electro-magnetic environments and hence relaxations of each proton.

1,4-Bis(methylcyclohexyl ether)-2,5-dibromomethylbenzene (1). **1** was prepared and purified as detailed elsewhere.[34] ^{1}H NMR (C_6D_6, ambient temperature): 6.57 (s, 2 H), 4.36 (s, 4 H), 3.42 (d, J = 6.4 Hz, 4 H), 1.9−1.5 (m, 12 H), and 1.3−0.9 ppm (10 H). ^{13}C NMR (C_6D_6, ambient temperature): 151.1, 114.7, 74.2, 38.2, 30.1, 28.8, 26.8, and 26.2 ppm; peak expected at around 130 ppm due to phenyl*C*-CH_2Br was hidden by C_6D_6 peaks. Thus, confirmed in $CDCl_3$ where observed peaks at 150.7, 127.4, 114.5, 74.4, 37.9, 29.9, 28.8, 26.5, and 25.9 ppm.

Synthesis of Poly{(1,4-fullerene)-*alt*-[1,4-dimethylene-2,5-bis(cyclohexylmethyl ether)phenylene]} (PFDP). PFDPs were prepared following the general protocol given elsewhere.[34] Minor modifications were made to that process so the full details of a representative experiment are given here. In a 1000 mL vessel, C_{60} (1.0 g, 1.388 × 10^{-3} mol) and **1** (0.674 g, 1.388 × 10^{-3} mol) were dissolved in toluene (650 mL) at room temperature. CuBr (0.398 g, 2.775 × 10^{-3} mol) and bipyridine (0.867 g, 5.55 × 10^{-3} mol) were added and the temperature of the vigorously stirred mixture slowly raised to 110 °C. After 22 h, the mixture was reduced to *ca.* 100 mL by evaporation and dropped into THF (700 mL) to precipitate unreacted fullerene. Precipitates were then removed by passing the solution through a filtering column (*ca.* 2 cm of Brockmann I activated neutral 150 mesh alumina layered on top of *ca.* 15 cm of MN Kieselgel 60M, 230−400 mesh silica). The red solution was again reduced to around 100 mL by evaporation, dropped into THF (700 mL), and passed through a fresh column prepared as above detailed. Evaporation of the solvent left around 100 mL that was dropped into methanol (700 mL), to yield a brown precipitate. This was dissolved in toluene (100 mL), dropped into methanol, and recovered and rinsed with methanol over a glass frit. Drying under reduced pressure for 3 d at 40 °C gave a light-brown powder with a yield of 0.69 g, 48% (PFDP). ^{1}H NMR (400 MHz, C_6D_6, D1 = 10 s, 4096 scans, ambient temperature, and shown in Figure S2, Supporting Information): 7.24 (phenyl-*H*), 6.88 (phenyl-*H*), 4.43 (AB quartet, J = 9.6 Hz, −CH_2-Br), 4.17 (J = 126.8 Hz, 12.6 Hz, 1,4-C_{60}−CH_2−), 3.96 (dd, J = 6 Hz, 1.3 Hz, −O−CH_2−), 3.94 (m, −O−CH_2−), and broad peaks from 2.1 to 1.5 and 1.45 to 0.8 ppm (cyclohexyl-*H*). ^{13}C NMR (100 MHz, C_6D_6, D1 = 10 s, 8192 scans, ambient temperature, Figure 1): 158.69, 152.57, 152.13, 149.10, 148.94, 147.53, 147.34, 147.23, 146.87, 145.89, 145.37, 145.28, 145.04, 144.69, 144.64, 144.56, 144.22, 144.14, 143.54, 143.49, 143.38, 143.10, 142.88, 142.41, 142.32, 141.08, 139.34, and 138.07 (C_{60} sp^2) 118.15 (phenyl *C*−H), 115.15 (phenyl *C*−H), 75.54 (−*C*H_2−O−), 43.03 (C_{60}−*C*H_2−), 38.53 (−*C*H− cyclohexyl), 38.57 (−*C*H−), 30.46 (−*C*H_2−), 30.42 (−*C*H_2−), 30.40 (−*C*H_2−), 30.36 (−*C*H_2−), 28.95 (−*C*H_2Br−), 26.90 (−*C*H_2−), and 26.86 ppm (−*C*H_2−).

Synthesis of Poly(poly{(1,4-fullerene)-*alt*-[1,4-dimethylene-2,5-bis(cyclohexylmethyl ether)phenylene]}-*block*-poly(3-hexylthiophene)) (PFDP-*b*-P3HT). Albeit for the changes in molecular weights of the components polymers, and the accordingly proportional change in weights of materials used, the following method is representative. P3HT-**1** M_n (GPC) = 7965 g mol^{-1},

hence probable molecular weight,[31c] is closer to 4900 g mol^{-1} ($\approx$ 29 repeat units). The PFDP molecular weight distribution was dominated by an M_p around 9 repeat units (equivalent to $M_p \approx 9930$ g mol^{-1}). Thus, P3HT-**1** (85 mg, 1.7×10^{-5} mol), PFDP (170 mg, 1.7×10^{-5} mol) and 18-crown-6 (500 mg, 2.27×10^{-3} mol) were stirred at ambient temperature until dissolved in 75 mL toluene. A high excess of K_2CO_3 (4.8 g) was added, and then the mixture stirred at 75 °C for 22 h. The mixture was then passed through a silica column equipped with a glass frit to remove excess K_2CO_3 and aggregated material, washed with THF, and the collected solutions passed through a PTFE (0.45 μm) filter and dropped into methanol (1 L) to precipitate. The copolymer was washed with methanol, collected into a Schlenk thimble and washed repeatedly with water (100 mL) and 18-crown-6 (2 g) over a period of several days to further remove K_2CO_3. The copolymer was again reprecipitated from toluene (100 mL) with methanol (300 mL) and recovered by centrifuge to remove 18-crown-6. Drying under reduced pressure at room temperature for 3 days returned a black-purple powder, PFDP-*b*-P3HT-**1** (yield = 27%). GPC: see Table 1; ^{1}H NMR (400 MHz, dichlorobenzene-d_4, D1 = 10 s, Figure S10, Supporting Information), 7.2 (s, thiophene-*H*), 4.1, 3.9 (PFDP-*H*), 2.95 (P3HT, alkyl, α-*H*), 2.8 (chain-end group, alkyl, α−*H*), 2.7 (P3HT, chain-end group, alkyl, α−*H*, possibly adjacent to PFDP), 1.8 (P3HT-alkyl-*H*), 1.55 (P3HT-alkyl-*H*), 1.4 (P3HT-alkyl-*H*).

Acknowledgment. The authors warmly thank Nicolas Guidolin (LCPO, ENSCBP, France) for technical assistance, and Dr Stéphane Guillerez, Dr Noëlla Lemaitre (CEA, Bourget du Lac, France), and Dr Pierre Iratçabal (Université de Pau et les Pay de l'Adour, France) for helpful discussions. Dr Christelle Absalon (Centre d'Etude Structurale et d'Analyse des Molécules Organiques, Université de Bordeaux, France) is gratefully thanked for MALDI−TOF characterizations. Thanks are extended to the CNRS and the ANR through the "SOLCOP" research program, and to the GIS (Advanced Materials in Aquitaine) for funding R.C.H.

Supporting Information Available: Figures showing NMR spectra of PFDP, P3HT, and PFDP-*b*-P3HT-**1**, MALDI−TOF of P3HT-**1**, tracking PFDP-*b*-P3HT-**1** formation by GPC, DSC and fluorescence characterizations of PFDP, P3HT-**1** and PFDP-*b*-P3HT-**1**, and supplementary AFM images and profiles. This material is available free of charge via the Internet at http://pubs.acs.org.

References and Notes

(1) (a) Chen, X. L.; Jenekhe, S. A. *Macromolecules* **2000**, *33*, 4610. (b) Shklyarevskiy, I. O.; Jonkheijm, P.; Christianen, P. C. M.; Schenning, A. P. H. J.; Meijer, E. W.; Henze, O.; Kilbinger, A. F. M.; Feast, W. J.; Del Guerzo, A.; Desvergne, J.-P.; Maan, J. C. *J. Am. Chem. Soc.* **2005**, *127*, 1112. (c) Hiorns, R. C.; Holder, S. J. *Polym. Int.* **2009**, *58*, 323. (d) Sommerdijk, N. A. J.; Holder, S. J.; Hiorns, R. C.; Jones, R. G.; Nolte, R. J. M. *Macromolecules* **2000**, *33*, 8289. (e) Hiorns, R. C.; Holder, S. J.; Schué, F.; Jones, R. G. *Polym. Int.* **2001**, *50*, 1016.

(2) Mori, T.; Watanabe, T.; Minagawa, K.; Tanaka, M. *J. Polym. Sci. Pt A Polym. Chem.* **2005**, *43*, 1569. (b) Yu, L.; Li, W.; Wang, H.; Morkved, T. L.; Jaeger, H. M. *Macromolecules* **1999**, *32*, 3034. (c) Wang, H.; You, W.; Jiang, P.; Yu, L.; Wang, H. H. *Chem.—Eur. J.* **2004**, *10*, 986. (d) Hiorns, R. C.; Martinez, H. *Synth. Met.* **2003**, *139*, 463.

(3) (a) Günes, S.; Neugebauer, H.; Sariciftci, N. S. *Chem. Rev.* **2007**, *107*, 1324. (b) Thompson, B. C.; Fréchet, J. M. J. *Angew. Chem., Int. Ed.* **2008**, *47*, 58. (c) Helgesen, M.; Søndergaard, R.; C. Krebs, F. C. *J. Mater. Chem.* **2010**, *20*, 36.

(4) (a) Choi, M.-C.; Kim, Y.; Ha, C.-S. *Prog. Polym. Sci.* **2008**, *33*, 581. (b) Akcelrud, L. *Prog. Polym. Sci.* **2003**, *28*, 875.

(5) (a) Yesodha, S. K.; Pillai, C. K. S.; Tsutsumi, N. *Prog. Polym. Sci.* **2004**, *29*, 45. (b) Cho, M. J.; Choi, D. H.; Sullivan, P. A.; Akelaitis, A. J. P.; Dalton, L. R. *Prog. Polym. Sci.* **2008**, *33*, 1013. (c) Moliton, A. *Optoelectronics of molecules and polymers*; Springer: New York, 2005. (d) McCullochm, I.; Yoon, H. *Encycl. Mater.: Sci. Technol.* **2008**, 8476.

(6) (a) Ling, Q.-D.; Liaw, D.-J.; Zhu, C.; Chan, D. S.-H.; Kang, E.-T.; Neoh, K.-G. *Prog. Polym. Sci.* **2008**, *33*, 917. (b) Singh, Th. B.; Sariciftci, N. S.; Jaiswal, M.; Menon, R. In *Handbook of Organic Electronics and Photonics*; Nalwa, H. S., Ed.; 2008; Vol. *3*, p 153. (c) Singh, Th. B.; Sariciftci, N. S. *Annu Rev. Mater. Res.* **2006**, *36*, 199. (d) Dimitrakopoulos, C. D.; Mascaro, D. J. *IBM J. Res. Dev.* **2001**, *45*, 11. (e) Fréchet, J. M. J. *Prog. Polym. Sci.* **2005**, *30*, 844.

(7) Guimard, N. K.; Gomez, N.; Schmidt, C. E. *Prog. Polym. Sci.* **2007**, *32*, 876.

(8) (a) Mikroyannidis, J. A.; Spiliopoulos, I. K.; Kasimis, T. S.; Kulkarni, A. P.; Jenekhe, S. A. *Macromolecules* **2003**, *36*, 9295. (b) Olsen, B. D.; Segalman, R. A. *Macromolecules* **2005**, *38*, 10127. (c) Cui, J.; Zhu, J.; Ma, Z.; Jiang, W. *Chem. Phys.* **2006**, *321*, 1. Klok, H.-A.; Lecommandoux, S. *Adv. Mater.* **2001**, *13*, 1217. (d) Kallitsis, J.; Tsolakis, P.; Andreopoulou, A. *Semiconducting Polymers, Chemistry, Physics and Engineering*; Hadziioannou, G., Malliaras, G. G., Eds.; Wiley-VCH: Weinheim, Germany, 2006; Chapter 2, Vol, *1*. (e) Malliaras, G. G.; Hadziioannou, G.; Herrema, J. K.; Wildeman, J.; Wieringa, R. H.; Gill, R. E.; Lampoura, S. S. *Adv. Mater.* **1993**, *5*, 721.

(9) (a) Dennler, G.; Scharber, M. C.; Brabec, C. J. *Adv. Mater.* **2009**, *21*, 1. (b) Park, S. H.; Roy, A.; Beaupré, S.; Cho, S.; Coates, N.; Moon, J. S.; Moses, D.; Leclerc, M.; Lee, K.; Heeger, A. J. *Nature Photon.* **2009**, *3*, 297. (c) Campoy-Quiles, M.; Ferenczi, T.; Agostinelli, T.; Etchegoin, P. G.; Kim, Y.; Anthopoulos, T. D.; Stavrinou, P. N.; Bradley, D. D. C.; Nelson, J. *Nat. Mater.* **2008**, *7*, 158.

(10) (a) Chen, H.-Y.; Hou, J.; Zhang, S.; Liang, Y.; Yang, G.; Yang, Y.; Yu, L.; Wu, Y.; Li, G. *Nat. Photonics* **2009**, *3*, 3649. (b) Park, S. H.; Roy, A.; Beaupré, S.; Cho, S.; Coates, N.; Moon, J. S.; Moses, D.; Leclerc, M.; Lee, K.; Heeger, A. J. *Nat. Photonics* **2009**, *3*, 297. (c) Liang, Y.; Xu, Z.; Xia, J.; Tsai, S.-T.; Wu, Y.; Li, G.; Ray, C.; Yu, L. *Adv. Mater.* (ASAP) DOI: 10.1002/adma.200903528.

(11) (a) Kirova, N. *Polym. Int.* **2007**, *57*, 678. (b) Cook, S.; Liyuan, H.; Furube, A.; Katoh, R. *J. Phys. Chem. C* (ASAP) DOI: 10.1021/jp101340b.

(12) (a) Jaiswal, M.; Menon, R. *Polym. Int.* **2006**, *55*, 1371. (b) Moliton, A.; Nunzi, J.-M. *Polym. Int.* **2006**, *55*, 583. (c) Moliton, A.; Hiorns, R. C. *Polym. Int.* **2004**, *53*, 1397. (d) Nunzi, J.-M. *C. R. Physique* **2002**, *3*, 523. (e) Sariciftci, N. S.; Smilowitz, L.; Heeger, A. J.; Wudl, F. *Science* **1992**, *258*, 1474.

(13) (a) Darling, S. B. *Energy Environ. Sci.* **2009**, *2*, 1266. (b) Botiz, I.; Darling, S. B. *Mater. Today* **2010**, *13* (5), 42.

(14) Watkins, P. K.; Walker, A. B.; Verschoor, G. L. B. *Nano Lett.* **2005**, *5*, 1814.

(15) Sun, S.; Fan, Z.; Wang, Y.; Haliburton, J. *J. Mater. Sci.* **2005**, *40*, 1429.

(16) Gratt, J. A.; Cohen, R. E. *J. Appl. Polym. Sci.* **2004**, *91*, 3362.

(17) Sun, S.-S. *Solar Energy Mater. Solar Cells* **2003**, *79*, 257.

(18) de Boer, B.; Stalmach, U.; van Hutten, P. F.; Melzer, C.; Krasnikov, V. V.; Hadziioannou, G. *Polymer* **2001**, *42*, 9097.

(19) Hiorns, R. C.; Iratçabal, P.; Bégué, D.; Khoukh, A.; de Bettignies, R.; Leroy, J.; Firon, M.; Sentein, C.; Martinez, H.; Preud'homme, H.; Dagron-Lartigau, C. *J. Polym. Sci., Part A: Polym. Chem.* **2009**, *47*, 2304.

(20) Lindner, S. M.; Hüttner, S.; Chiche, A.; Thelakkat, M.; Krausch, G. *Angew. Chem., Int. Ed.* **2006**, *45*, 3364.

(21) (a) Halls, J. J. M.; Walsh, C. A.; Greenham, N. C.; Marseglia, E. A.; Friend, R. H.; Moratti, S. C.; Holmes, A. B. *Nature* (*London*) **1995**, *376*, 498. (b) Yu, G.; Heeger, A. J. *J. Appl. Phys.* **1995**, *78*, 4510.

(22) Sun, S.-S.; Zhang, C.; Ledbetter, A.; Choi, S.; Seo, K.; Bonner, C. E., Jr.; Drees, M.; Sariciftci, N. S. *Appl. Phys. Lett.* **2007**, *90*, 043117.

(23) van der Veen, M. H.; de Boer, B.; Stalmach, U.; van de Wetering, K. I.; Hadziioannou, G. *Macromolecules* **2004**, *37*, 3673.

(24) Sivula, K.; Ball, Z. T.; Watanabe, N.; Fréchet, J. M. J. *Adv. Mater.* **2006**, *18*, 206.

(25) Barrau, S.; Heiser, T.; Richard, F.; Brochon, C.; Ngov, C.; van de Wetering, K.; Hadziioannou, G.; Anokhin, D. V.; Ivanov, D. A. *Macromolecules* **2008**, *41*, 2701.

(26) Sommer, M.; Lang, A. S.; Thelakkat, M. *Angew. Chem., Int. Ed.* **2008**, *47*, 7901.

(27) Tao, Y.; McCulloch, B.; Kim, S.; Segalman, R. A. *Soft Matter* **2009**, *5*, 4219.

(28) Zhang, Q.; Cirpan, A.; Russell, T. P.; Emrick, T. *Macromolecules* **2009**, *42*, 1079.

(29) Heiser, T.; Adamopoulos, G.; Brinkmann, M.; Giovanella, U.; Ould-Saad, S.; Brochon, C.; van de Wetering, K.; Hadziioannou, G. *Thin Solid Films* **2006**, *511−512*, 219.

(30) (a) Yokoyama, A.; Miyakoshi, R.; Yokozawa, T. *Macromolecules* **2004**, *37*, 1169. (b) Sheina, E. E.; Liu, J.; Iovu, M. C.; Darin W. Laird, D. W.; McCullough, R. D. *Macromolecules* **2004**, *37*, 3526. (c) Yokozawa, T.; Yokoyama, A. *Chem. Rev.* **2009**, *109* (11), 5595. (d) Hiorns, R. C.; de Bettignies, R.; Leroy, J.; Bailly, S.; Firon, M.; Sentein, C.; Khoukh, A.; Preud'homme, H.; Dagron-Lartigau, C. *Adv. Funct. Mater.* **2006**, *16*, 2263.
(31) (a) Jeffries-El, M.; Sauvé, G.; McCullough, R. D. *Macromolecules* **2005**, *38*, 10346. (b) Liu, J.; McCullough, R. D. *Macromolecules* **2002**, *35*, 9882. (c) Liu, J.; Loewe, R. S.; McCullough, R. D. *Macromolecules* **1999**, *32*, 5777. (d) Bronstein, H. A.; Luscombe, C. K. *J. Am. Chem. Soc.* **2009**, *131*, 12894. (e) Kaul, E.; Senkovskyy, V.; Tkachov, R.; Bocharova, V.; Komber, H.; Stamm, M.; Kiriy, A. *Macromolecules* **2010**, *43*, 77. (f) Hiorns, R. C.; Khoukh, A.; Gourdet, B.; Dagron-Lartigau, C. *Polym. Int.* **2006**, *55*, 608.
(32) Lan, Y.-K.; Yang, C. H.; Yang, H.-C. *Polym. Int.* **2010**, *59*, 16.
(33) (a) Brinkmann, M.; Rannou, P. *Macromolecules* **2009**, *42*, 1125. (b) Zen, A.; Saphiannikova, M.; Neher, D.; Grenzer, J.; Grigorian, S.; Pietsch, U.; Asawapirom, U.; Janietz, S.; Scherf, U.; Lieberwirth, I.; Wegner, G. *Macromolecules* **2006**, *39*, 2162. (c) Kline, R. J.; McGehee, M. D.; Kadnikova, E. N.; Liu, J.; Fréchet, J. M. J.; Toney, M. F. *Macromolecules* **2005**, *38*, 3312.
(34) Hiorns, R. C.; Cloutet, E.; Ibarboure, E.; Vignau, L.; Lemaitre, N.; Guillerez, S.; Absalon, C.; Cramail, H. *Macromolecules* **2009**, *42*, 3549.
(35) Hoeben, F. J. M.; Jonkheijm, P.; Meijer, E. W.; Schenning, A. P. H. J. *Chem. Rev.* **2005**, *105*, 1491.
(36) (a) Sun, S.; Fan, Z.; Wang, Y.; Haliburton, J. *J. Mater. Sci.* **2005**, *40*, 1429. (b) Zhang, C.; Choi, S.; Haliburton, J.; Cleveland, T.; Li, R.; Sun, S.-S.; Ledbetter, A.; Bonner, C. E. *Macromolecules* **2006**, *39*, 4317.
(37) (a) Giacalone, F.; Martín, N. *Chem. Rev.* **2006**, *106*, 5136. (b) Gogel, A.; Belik, P.; Walter, M.; Kraus, A.; Harth, E.; Wagner, M.; Spickermann, J.; Müllen, K. *Tetrahedron* **1996**, *52*, 5007. (c) Shi, S.; Khemani, K. C.; Li, Q. "C."; Wudl, F. *J. Am. Chem. Soc.* **1992**, *114*, 10656. (d) Ito, H.; Ishida, Y.; Saigo, K. *Tetrahedron Lett.* **2006**, *47*, 3095.
(38) Kadish, K. M.; Gao, X.; Van Caemelbecke, E.; Suenobu, T.; Fukuzumi, S. *J. Phys. Chem. A.* **2000**, *104*, 3878.
(39) Kadish, K. M.; Gao, X.; Van Caemelbecke, E.; Hirasaka, T.; Suenobu, T.; Fukuzumi, S. *J. Phys. Chem. A.* **1998**, *102*, 3898.
(40) Subramanian, R.; Kadish, K. M.; Vijayashree, M. N.; Gao, X.; Jones, M. T.; Miller, M. D.; Krause, K. L.; Suenobu, T.; Fukuzumi, S. *J. Phys. Chem.* **1996**, *100*, 16327.
(41) Miki, S.; Kitao, M.; Fukunishi, K. *Tetrahedron Lett.* **1996**, *37*, 2049.
(42) Smith, A. B., III; Strongin, R. M.; Brard, L.; Furst, G. T.; Romanow, W. J.; Owens, K. G.; Goldschmidt, R. J.; King, R. C. *J. Am. Chem. Soc.* **1995**, *117*, 5492.
(43) Audouin, F.; Nuffer, R.; Mathis, C. *J. Polym. Sci., Part A: Polym. Chem.* **2004**, *42*, 3456.
(44) Otsubo, T.; Aso, Y.; Takimiya, K.; Nakanishi, H.; Sumi, N. *Synth. Met.* **2003**, *133*, 325.
(45) Wohlgenannt, M.; Jiang, X. M.; Vardeny, Z. V.; Janssen, R. A. J. *Phys. Rev. Lett.* **2002**, *88*, 197401.
(46) Hiorns, R. C.; de Bettignies, R.; Leroy, J.; Bailly, S.; Firon, M.; Sentein, C.; Preud'homme, H.; Dagron-Lartigau, C. *Eur. Phys. J. Appl. Phys.* **2007**, *36*, 295.
(47) Bates, F. S.; Fredrickson, G. H. *Phys. Today* **1999**, *52*, 32.
(48) Segalman, R. A. *Mater. Sci. Eng. R* **2005**, *48*, 191.
(49) (a) Segalman, R. A.; McCulloch, B.; Kirmayer, S.; Urban, J. J. *Macromolecules* **2009**, *42*, 9205. (b) Klok, H.-A.; Lecommandoux, S. *Adv. Mater.* **2001**, *13*, 1217. (c) Lee, M.; Cho, B.-K.; Zin, W. C. *Chem. Rev.* **2001**, *101*, 3869.
(50) Brinkmann, M.; Rannou, P. *Macromolecules* **2009**, *42*, 1125.
(51) Brinkmann, M.; Wittmann, J.-C. *Adv. Mater.* **2006**, *18*, 860.
(52) Nakanishi, T.; Miyashita, N.; Michinobu, T.; Wakayama, Y.; Tsuruoka, T.; Ariga, K.; Kurth, D. G. *J. Am. Chem. Soc.* **2006**, *128*, 6328.
(53) Sayar, M.; Stupp, S. I. *Macromolecules* **2001**, *34*, 7135.
(54) Taton, D.; Angot, S.; Gnanou, Y.; Wolert, E.; Setz, S.; Duran, R. *Macromolecules* **1998**, *31*, 6030.
(55) Ederlé, Y.; Mathis, C.; Nuffer, R. *Synth. Met.* **1997**, *86*, 2287.
(56) Ederlé, Y.; Mathis, C. *Fullerene Sci. Technol.* **1996**, *4*, 1177.
(57) Wooley, K. L.; Hawker, C. J.; Fréchet, J. M. J.; Wudl, F.; Srdanov, G.; Shi, S.; Li, C.; Kao, M. *J. Am. Chem. Soc.* **1993**, *115*, 9836.
(58) Schwalm, T.; Wiesecke, J.; Immel, S.; Rehahn, M. *Macromolecules* **2007**, *40*, 8842.
(59) Hontis, L.; Vrindts, V.; Lutsen, L.; Vanderzande, D.; Gelan, J. *Polymer* **2001**, *42*, 5793.
(60) Ng, S. C.; Xu, J. M.; Chan, H. S. O. *Synth. Met.* **2000**, *110* (1), 31.
(61) Chambon, S.; Rivaton, A.; Gardette, J.-L.; Firon, M. *Solar Energy Mater. Solar Cells* **2007**, *91*, 394.
(62) Ouhib, F.; Hiorns, R. C.; de Bettignies, R.; Bailly, S.; Desbrières, J.; Dagron-Lartigau, C. *Thin Solid Films* **2008**, *516*, 7199.
(63) *Polymers: Chemistry and Physics of Modern Materials*, 3rd ed., Cowie, J. M. G.; Arrighi, V. CRC Press, Taylor and Francis Group: Boca Raton, FL, 2008.
(64) (a) Müller, C.; Radano, C. P.; Smith, P.; Stingelin-Stutzmann, N. *Polymer* **2008**, *49*, 3973. (b) Wunderlich, B.; Dole, M. *J. Polym. Sci.* **1957**, *24*, 201. (c) Malik, S.; Nandi, A. K. *J. Polym. Sci., Part B: Polym. Phys.* **2002**, *40*, 2073. (d) Zhang, Y.; Tajima, K.; Hashimoto, K. *Macromolecules* **2009**, *42*, 7008.
(65) Trznadel, M.; Pron, A.; Zagorska, M.; Chrzaszcz, R.; Pielichowski, J. *Macromolecules* **1998**, *31*, 5051.
(66) Zhang, T.-H.; Lu, P.; Wang, F.; Wang, G.-W. *Org. Biomol. Chem.* **2003**, *1*, 4403.
(67) Fery-Forgues, S.; Lavabe, D. *J. Chem. Educ.* **1999**, *76*, 1260.
(68) Qian, J.; Zhang, M.; Manners, I.; Winnik, M. A. *Trends Biotechnol.* **2010**, *28* (2), 84.
(69) Urien, M.; Erothu, H.; Cloutet, E.; Hiorns, R. C.; Vignau, L.; Cramail, H. *Macromolecules* **2008**, *41*, 7033.